OBESITY

Early-set POMC methylation variability is accompanied by increased risk for obesity and is addressable by MC4R agonist treatment

Lara Lechner[1], Robert Opitz[2], Matt J. Silver[3], Philipp M. Krabusch[1], Andrew M. Prentice[3], Martha S. Field[4], Harald Stachelscheid[5], Elsa Leitão[6], Christopher Schröder[6], Valeria Fernandez Vallone[5], Bernhard Horsthemke[6], Karl-Heinz Jöckel[7], Börge Schmidt[7], Markus M. Nöthen[8], Per Hoffmann[8], Stefan Herms[8], Patrick W. Kleyn[9], Matthias Megges[1], Ulrike Blume-Peytavi[10], Katja Weiss[11], Knut Mai[12,13], Oliver Blankenstein[1,14], Benedikt Obermayer[15], Susanna Wiegand[16], Peter Kühnen[1]*

Increasing evidence points toward epigenetic variants as a risk factor for developing obesity. We analyzed DNA methylation of the *POMC* (pro-opiomelanocortin) gene, which is pivotal for satiety regulation. We identified sex-specific and nongenetically determined *POMC* hypermethylation associated with a 1.4-fold (confidence interval, 1.03 to 2.04) increased individual risk of developing obesity. To investigate the early embryonic establishment of *POMC* methylation states, we established a human embryonic stem cell (hESC) model. Here, hESCs (WA01) were transferred into a naïve state, which was associated with a reduction of DNA methylation. Naïve hESCs were differentiated via a formative state into POMC-expressing hypothalamic neurons, which was accompanied by re-establishment of DNA methylation patterning. We observed that reduced *POMC* gene expression was associated with increased *POMC* methylation in *POMC*-expressing neurons. On the basis of these findings, we treated *POMC*-hypermethylated obese individuals ($n = 5$) with an MC4R agonist and observed a body weight reduction of 4.66 ± 2.16% (means ± SD) over a mean treatment duration of 38.4 ± 26.0 weeks. In summary, we identified an epigenetic obesity risk variant at the *POMC* gene fulfilling the criteria for a metastable epiallele established in early embryonic development that may be addressable by MC4R agonist treatment to reduce body weight.

INTRODUCTION

The increasing prevalence of obesity with associated comorbidities of cardiovascular disease and diabetes mellitus type 2 poses a severe burden for health care systems globally. The World Health Organization (WHO) has made reducing the prevalence of obesity one of its major goals (*1*, *2*). It is therefore important to identify the risk factors and mechanisms underlying body weight regulation that predispose an individual to develop obesity, with the goal of establishing urgently needed new therapies and prevention strategies.

The reported concordance of body mass index (BMI) in monozygotic (MZ) twins is between 40 and 70%, suggesting that genetic background might play a major role in body weight regulation (*3*). However, patients with monogenic obesity are rare, with the majority of identified mutations in genes related to the leptin-melanocortin pathway (*4*). Additional genetic variants that predict an individual's predisposition to gain weight and develop obesity have been combined into a polygenic risk score (*5*), yet, so far, identified genetic risk variants explain less than 25% of inter-individual body weight variability. The failure to identify genetic variants that explain the high BMI concordance observed in MZ twins has been termed missing heritability (*6*), and it has been hypothesized that epigenetic variants might additionally contribute to an individual's risk of developing obesity. This is supported by studies in plants and mammals in which variability of epigenetic modifications such as DNA methylation affects phenotypic variation.

Epigenetically driven phenotypic variation has been described in eusocial insect morphs (polyphenisms) including honey bees, ants,

[1]Department of Pediatric Endocrinology, Charité–Universitätsmedizin Berlin, corporate member of Freie Universität Berlin, Humboldt-Universität zu Berlin, and Berlin Institute of Health, 13353 Berlin, Germany. [2]Institute for Experimental Pediatric Endocrinology, Charité–Universitätsmedizin Berlin, corporate member of Freie Universität Berlin, Humboldt-Universität zu Berlin, and Berlin Institute of Health, 13353 Berlin, Germany. [3]Medical Research Council Unit, Gambia at the London School of Hygiene and Tropical Medicine, Fajara, Banjul, PO Box 273, Gambia. [4]Division of Nutritional Sciences, Cornell University, Ithaca, NY 14850, USA. [5]Berlin Institute of Health, corporate member of Freie Universität Berlin and Humboldt-Universität zu Berlin, BIH Core Unit Stem Cells and Organoids, 13353 Berlin, Germany. [6]Institute of Human Genetics, University Hospital Essen, 45147 Essen, Germany. [7]Institute of Medical Informatics, Biometry and Epidemiology, University Hospital Essen, 45147 Essen, Germany. [8]Institute of Human Genetics, School of Medicine and University Hospital Bonn, University of Bonn, 53127 Bonn, Germany. [9]Rhythm Pharmaceuticals, Boston, MA 02116, USA. [10]Clinical Research Center for Hair and Skin Science, Department of Dermatology and Venerology and Allergology, Charité-Universitätsmedizin Berlin, corporate member of Freie Universität Berlin, and Humboldt-Universität zu Berlin, 10117 Berlin, Germany. [11]Klinik für Angeborene Herzfehler – Kinderkardiologie, Deutsches Herzzentrum der Charité, Charité–Universitätsmedizin Berlin, corporate member of Freie Universität Berlin, Humboldt-Universität zu Berlin, and Berlin Institute of Health, 13353 Berlin, Germany. [12]Department of Endocrinology, Diabetes, and Nutrition and Charité Center for Cardiovascular Research, Charité–Universitätsmedizin Berlin, corporate member of Freie Universität Berlin, Humboldt-Universität zu Berlin, and Berlin Institute of Health, 10117 Berlin, Germany. [13]German Center for Diabetes Research, 85764 München-Neuherberg, Germany. [14]Department Endocrinology and Metabolism, Labor Berlin-Charité Vivantes GmbH, 13353 Berlin, Germany. [15]Core Unit Bioinformatics (CUBI), Berlin Institute of Health/Charité– Universitätsmedizin Berlin, corporate member of Freie Universität Berlin, Humboldt-Universität zu Berlin, and Berlin Institute of Health, 10117 Berlin, Germany. [16]Charité-Universitätsmedizin Berlin, corporate member of Freie Universität Berlin, Humboldt-Universität zu Berlin, Center for Social-Pediatric Care/Pediatric Endocrinology and Diabetology, 13353 Berlin, Germany.
*Corresponding author. Email: peter.kuehnen@charite.de

and inbred animal models (*7*). The variable response of genetically identical mouse strains exposed to a high-fat diet is an additional example of the nongenetic regulation of phenotypic changes (*8*). Further evidence comes from animal models including agouti viable yellow (A^{vy}) and axin fused ($Axin^{Fu}$) mice, in which DNA methylation changes at regions known as metastable epialleles are associated with phenotypic variation (*9*, *10*). Metastable epialleles are regions where DNA methylation is established stochastically during embryonic development, and this methylation is invariable across cell types and is stable over time (*11*). Putative metastable epialleles have recently been identified in humans, and we provided evidence that a variable methylated region (VMR) of the *POMC* (pro-opiomelanocortin) gene might be a metastable epiallele that is influenced by certain nutritional factors around the time of conception (*12*).

POMC is embedded in the leptin-melanocortin signaling cascade where the hormone leptin, secreted by adipocytes, activates POMC-expressing neurons within the hypothalamic arcuate nucleus. This, in turn, leads to the generation and secretion of POMC-derived peptides such as α- and β-MSH (melanocyte-stimulating hormone). Both peptides can activate the MC4R (melanocortin 4 receptor) within the paraventricular nucleus, thereby regulating satiety and alterating energy expenditure. Genetic defects within this cascade lead to severe hyperphagia and early-onset obesity.

Recently, the MC4R agonist setmelanotide has been approved by the U.S. Food and Drug Administration (FDA) as a pharmacological treatment option for patients with mutations in the genes *POMC*, *PCSK1* (proprotein convertase subtilisin/ kexin type 1), or *LEPR* (leptin receptor) (*13*). We recently investigated links between epigenetic variation and risk for obesity development and demonstrated increased DNA methylation at the *POMC* VMR in obese adolescents and adults (*12*, *14*).

On the basis of these earlier findings, in this study, we investigated the extent to which *POMC* VMR methylation affects individual risk of obesity, the potential for a MC4R agonist as a pharmacological treatment option for carriers of an epigenetic *POMC* variant, the potential influence of environmental or nutritional factors on the establishment of variable methylation states in differentiating hypothalamic neurons in the early embryo, and the links between *POMC* methylation variability and differences in *POMC* expression.

RESULTS

POMC methylation is established in the early embryo and is associated with obesity in females

In previous studies, we analyzed *POMC* methylation in peripheral blood cells and MSH-positive hypothalamic postmortem human neurons and identified increased *POMC* methylation in a CpG island at the intersection between *POMC* intron 2 and coding exon 3 (hg38 chr2:25,161,767–25,161,685) in obese compared with non-obese individuals (Fig. 1A and fig. S1A) (*12*, *14*). A large number of identified DNA methylation differences are driven by genetic variants, especially in cis, which would not qualify as primary epigenetic variants (*15*). Therefore, to evaluate genetic influences on *POMC* DNA methylation, we performed genome-wide association studies (GWAS) using single-nucleotide polymorphism (SNP) genotypes from blood samples of 1128 individuals originating from the longitudinal Heinz-Nixdorf-Recall (HNR) study (table S1) (*16*), for which IlluminaHumanMethylation450K BeadChip methylation data were available. Because none of the nine CpGs within the *POMC* VMR region is represented by the IlluminaHumanMethylation450K BeadChip, we first analyzed six CpGs covered by the array flanking the *POMC* region (fig. S1) and observed that for five of them, methylation was associated with SNPs in the *EFR3B-POMC* locus (fig. S2). For the nine CpGs within the *POMC* VMR, DNA methylation was determined by pyrosequencing blood DNA samples from the HNR study for which SNP genotypes were available (n = 1083) (*16*). We observed that methylation at intronic *POMC* CpG positions −2 and −1 was influenced by SNPs in the *EFR3B-POMC* region (rs13428823, rs17046887, and rs934778; Fig. 1B and fig. S1, B and C). In all other *POMC* CpG positions (CpG positions +1 to +7), DNA methylation was not associated with any genetic variation in cis or trans (Fig. 1B and fig. S1C). Subsequent DNA methylation analysis focused on these seven exonic CpGs where methylation was not genetically determined.

Further analysis of the HNR cohort revealed a sex-specific *POMC* methylation pattern with increased mean methylation in females compared with males {Tukey post hoc test, mean difference [95% confidence interval (CI)] = 5.357 (4.16–6.56), $P < 0.0001$} and increased mean methylation in severely obese (BMI > 35 kg/m^2) compared with overweight and moderately obese (BMI between 25 and 35 kg/m^2) participants [Tukey post hoc test, mean difference (95% CI) = 2.073 (0.32–3.28), $P = 0.016$] (Fig. 2A). Moreover, we identified significantly increased *POMC* DNA methylation in obese (BMI > 35 kg/m^2) compared with normal-weight female participants [Tukey post hoc test, mean difference (95% CI) = 2.934 (0.33–5.54), $P = 0.023$] (Fig. 2A). In detail, the increase of *POMC* methylation was present at all VMR CpG positions except for CpG positions +3 and +5 (Fig. 2B). For *POMC* CpG positions +1 to +7, the distribution of *POMC* methylation variability was shifted toward higher methylation in obese female (BMI > 35 kg/m^2) individuals (Fig. 2C). Elevated *POMC* methylation was associated in female individuals with an increased risk of obesity with an odds ratio of 1.44 (95% Cl 1.03–2.04) (Fig. 2D).

POMC is a putative metastable epiallele with methylation established in the early embryo (*12*). Analysis of twin cohort methylation data can therefore provide insights into the timing of DNA methylation establishment (*17*). MZ twins originate from identical cells in the early embryo and are therefore exposed to the same epigenetic regulatory network before embryo cleavage, leading to locus-specific epigenetic supersimilarity (ESS) (*17*). In contrast, for dizygotic (DZ) twins, early DNA methylation establishment occurs separately at the cellular level despite twins sharing the same womb.

We analyzed *POMC* methylation at CpG positions +1 to +7 in MZ (n = 32) and DZ (n = 38) twins. We identified high methylation concordance in MZ twins ($r = 0.78$, $P < 0.0001$) (Fig. 2E), in contrast to DZ twins, where no correlation ($r = 0.31$, $P = 0.0582$) was observed (Fig. 2F). Notably, we observed an intratwin correlation of DNA methylation of each twin pair in both MZ ($r = 0.71$, $P < 0.0001$) and DZ ($r = 0.34$, $P = 0.0389$) twins for *POMC* CpG positions −2 and − 1, which are both influenced by genetic variants (figs. S3, A and B, and S4, A and B). As a control experiment, we analyzed the metastable epiallele *PAX8* (paired box protein 8), for which we observed similar results, with a high intratwin correlation in MZ compared with DZ twins (fig. S3, C and D). These data support the hypothesis that *POMC* VMR exhibits ESS, with locus-

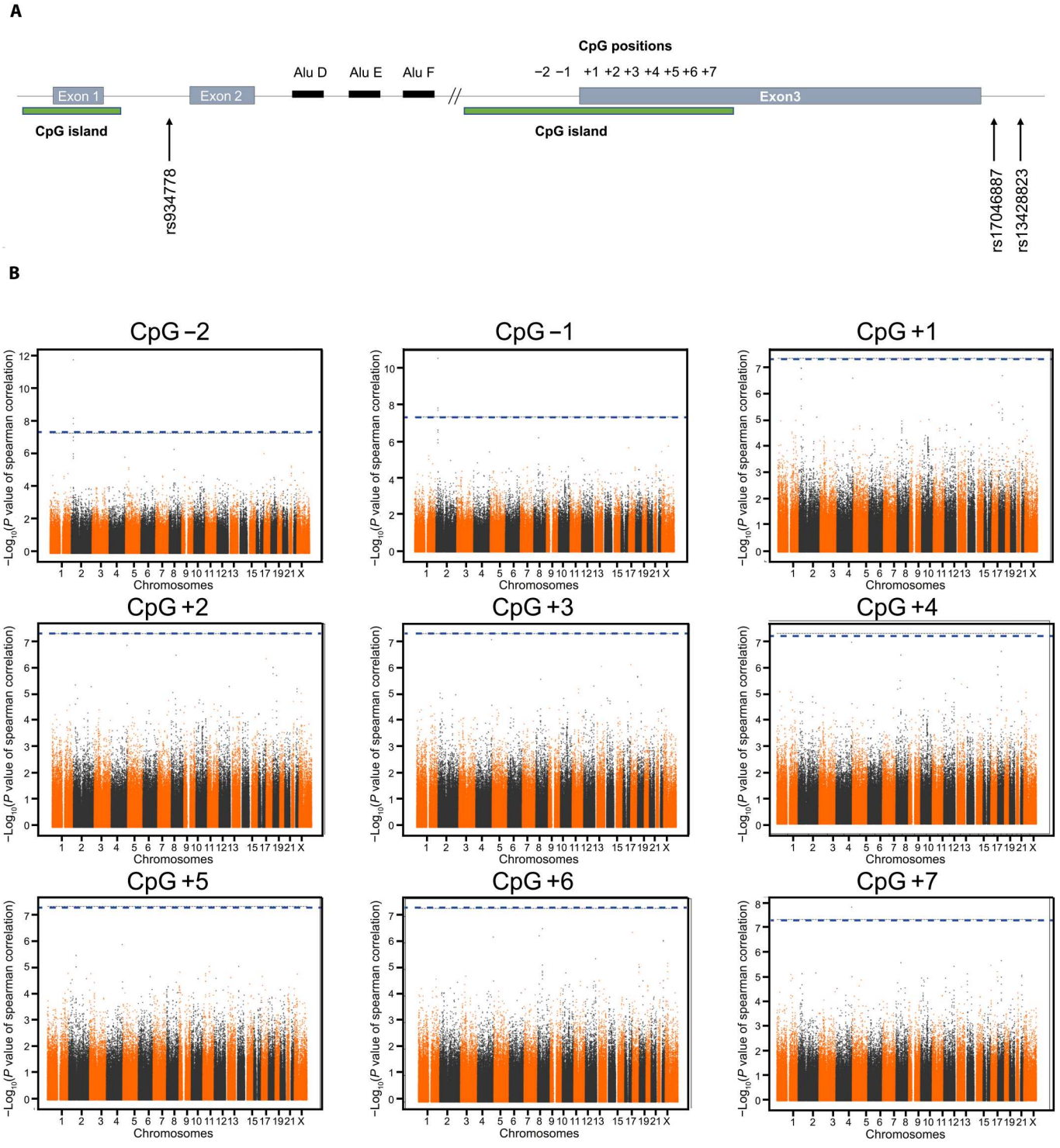

Fig. 1. *POMC* VMR methylation is not genetically determined. (**A**) Schematic illustration of the human *POMC* region and *POMC* VMR (hg38 chr2:25,161,767–25,161,685) including localization of primate specific Alu elements (Alu D-F). (**B**) Manhattan plots of genotype analysis using SNP genotypes and CpG methylation data for *POMC* CpG positions −2 to +7. Horizontal lines represent the GWAS significance threshold [*P* value of 5×10^{-8} equivalent to 7.3 on the $-\log_{10}(P)$ scale].

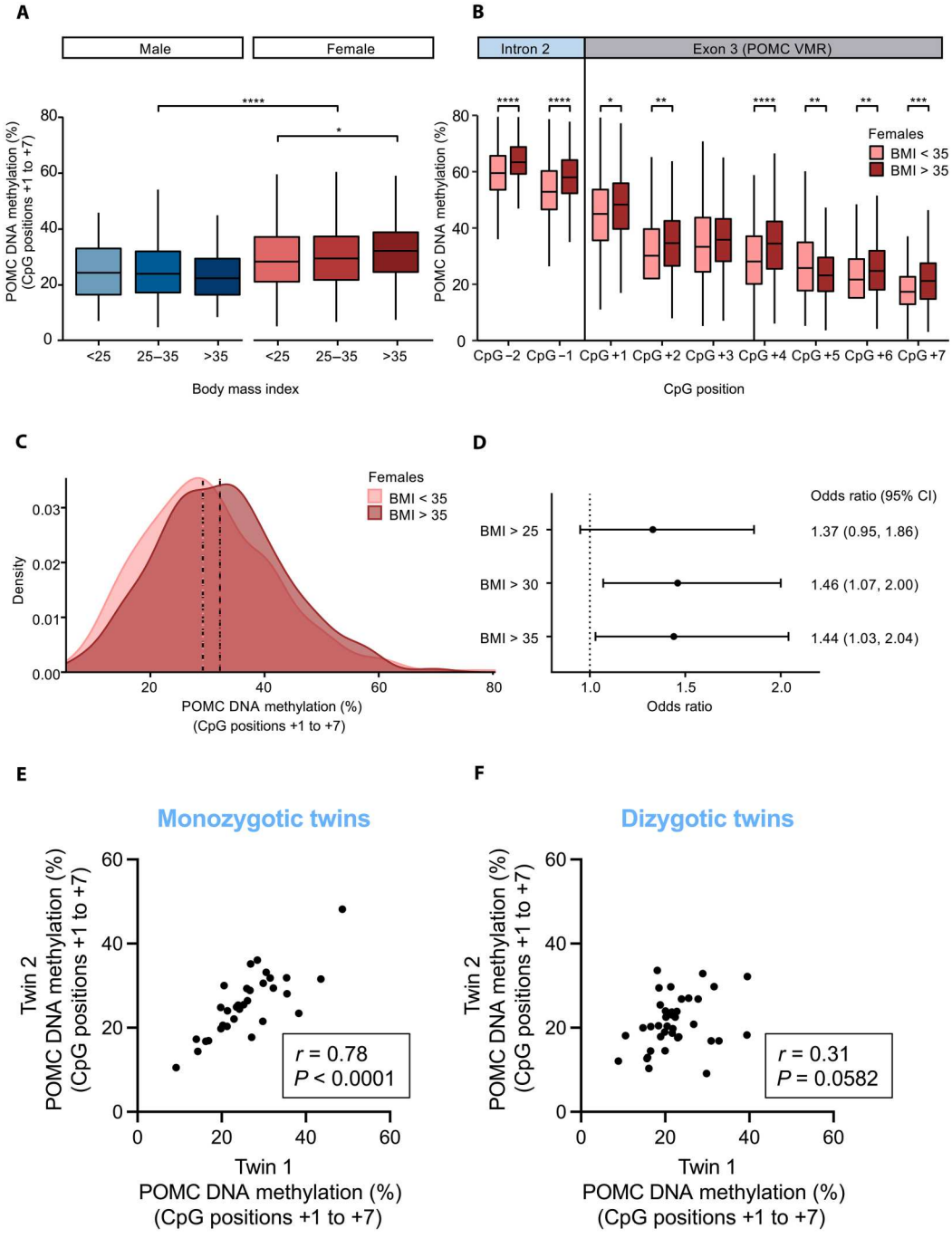

Fig. 2. Sex-specific *POMC* hypermethylation in individuals with obesity. (**A**) DNA methylation analysis of a *POMC* metastable epiallele region in the HNR cohort (n = 1383) reveals sex-specific methylation differences. Two-way ANOVA with BMI groups and sex as factors revealed a significant difference in DNA methylation between the BMI groups (F = 3.851, P = 0.0215) and between sex (F = 80.923, P = <0.0001). Subsequent one-way ANOVA for each sex group revealed significant BMI group differences in females (F = 3.891, P = 0.0209), but not in men (F = 0.166, P = 0.847). Mean methylation at CpG positions +1 to +7 in female individuals with obesity (BMI > 35 kg/m^2, n = 202) was significantly increased compared with normal-weight women (BMI below 25 kg/m^2, n = 209) [Tukey post hoc test, mean difference (95% CI) = 2.934 (0.33–5.54), P = 0.023]. (**B**) Separated for each CpG position, in female individuals with a BMI above 35 kg/m^2 (n = 202), methylation was significantly increased compared with females with a BMI below 35 kg/m^2 (n = 497) at all analyzed CpGs, with the exception of *POMC* CpG positions +3 and + 5. Statistical analysis was performed using Student's t test with Holms adjustment for multiple testing. Boxplots display median [interquartile range (IQR)]. (**C**) Distribution of *POMC* methylation at CpG positions +1 to +7 was shifted in obese compared with normal-weight female study participants, leading to a bimodal dispersion. Dotted lines show the median methylation for each group. (**D**) *POMC* methylation categorized into binomial factors by sex-specific median methylation (median = 29.7%). Significantly elevated odds ratios (ORs: high versus low methylation) suggest an association between high *POMC* methylation and obesity risk for female individuals with OR = 1.46 (risk for BMI > 30 kg/m^2) and OR = 1.44 (risk for BMI > 35 kg/m^2). (**E**) Pearson correlation of *POMC* VMR methylation (CpG positions +1 to +7) in MZ twins (n = 32) and (**F**) DZ twins (n = 38). Normality was tested with a Shapiro-Wilk test (MZ twin pairs: W = 0.97, P = 0.62; DZ twin pairs: W = 0.98, P = 0.67). *P < 0.05; **P < 0.01; ***P < 0.001; ****P < 0.0001.

specific establishment of DNA methylation occurring before embryo cleavage during twinning (*17*). ESS regions also show evidence of systematic interindividual variation, providing further evidence of early embryo establishment (*17*) and aligning with our observed *POMC* methylation results in the HNR cohort. In addition, ESS loci (and metastable epialleles more generally) may be influenced by the periconceptional environment, leading to a shift in the methylation distribution during early embryonic development (*17*–*19*). This observation, in combination with our finding that elevated *POMC* VMR methylation is associated with an increased risk of developing obesity in females, suggests that increased *POMC* methylation might interfere with the function of the leptin-melanocortin signaling pathway and that *POMC* methylation may be influenced by the periconceptional environment.

POMC expression and DNA methylation in hESCs during differentiation of hypothalamic neurons

On the basis of evidence that *POMC* DNA methylation variability affects body weight regulation, we wanted to gain further insights into the establishment of *POMC* DNA methylation during early embryonic development and investigate the functional consequences of *POMC* methylation variability. Human embryonic stem cells (hESCs) provide an opportunity to develop experimentally tractable in vitro models to examine DNA methylation patterns during early human development. To exploit these opportunities for studies of DNA methylation in the *POMC* region, we adopted previously published protocols for a stepwise differentiation of hESCs into POMC-expressing hypothalamic neurons (Fig. 3A) (*20*). Consistent with previous reports (*21*), culture of H1 hESCs (WA01) under these conditions resulted in differentiation of neuronal progenitors expressing high amounts of NKX2-1 (NK2 homeobox 1), a marker of both ventral telencephalic and hypothalamic neuronal progenitors, within 8 to 12 days of culture.

Upon further differentiation, cells adopted a neuronal morphology, and by day 26, cell cultures contained a high proportion of POMC-expressing neurons. Immunofluorescence analyses also showed active cellular POMC processing to derive α-MSH (Fig. 3, B and C, and fig. S5), and accumulation of desacetyl α-MSH was detected by liquid chromatography tandem mass spectrometry in media of POMC$^+$ neuronal cultures (Fig. 3D) (*22*).

Cell cultures harvested at different developmental stages for DNA methylation analysis showed high amounts of DNA methylation at the *POMC* locus in H1 hESCs at the start of our experiments (Fig. 3F). Differentiation of such primed H1 cells into hypothalamic NKX2-1$^+$ progenitors and POMC$^+$ neurons was then associated with only moderate gradual increases of DNA methylation at CpG positions +1 to +7. Thus, high DNA methylation in H1 hESCs limited their utility for studies of developmental changes in DNA methylation.

Although hESCs are originally derived from the inner cell mass (ICM) of the preimplantation epiblast, conventional hESCs including the H1 line are developmentally more advanced than their murine counterparts. They rather resemble the developmental state of mouse post-implantation epiblast and are therefore generally regarded as primed pluripotent (*23*, *24*). To achieve a developmental state more closely resembling the preimplantation epiblast with its associated DNA hypomethylation, we next used a previously described resetting method to derive vital naïve cells (*25*). Along with the observation of characteristic changes of cell morphology in reset cultures (Fig. 3A and fig. S6), immunofluorescence analysis of naïve cell cultures confirmed high expression of naïve epiblast-specific transcription factors (fig. S6) (*25*). When analyzing the transcriptome of primed H1 hESCs and derived naïve cells by single-cell RNA sequencing (RNA-seq) (fig. S7), we observed the expression of canonical pluripotency markers in both primed and naïve cells, whereas large clusters of cells expressing ICM markers were only found in naïve cell cultures (*26*).

Because naïve cells have pluripotent potential but a very low propensity to respond directly to inductive cues for somatic cell differentiation, we used a 14-day capacitation protocol (*27*) to transform naïve cells back into a formative state with pluripotent competence for somatic lineage induction (fig. S7). We next compared the efficiency of hypothalamic neuron differentiation for cell cultures starting with either primed H1 hESCs or capacitated cells. We found no gross differences, either in timing of cell differentiation or in the phenotype or transcriptome of the POMC neurons generated. This finding was further corroborated by benchmarking these neuronal cultures using single-cell RNA-seq (Fig. 3, G to I, and fig. S8).

DNA methylation at different cell states

The identification of an appropriate culture to differentiate POMC$^+$ neurons from naïve cells allowed us to perform a comparative analysis of developmental dynamics of DNA methylation at the *POMC* locus. In contrast to the high DNA methylation detected in primed H1 cells, naïve cells displayed a strong decrease in DNA methylation. Even after capacitation, DNA methylation at a formative state remained much lower compared with primed H1 cells (Fig. 3F). When capacitated cells were used for hypothalamic neuron differentiation, a marked increase in *POMC* DNA methylation was observed at the NKX2-1$^+$ neuronal progenitor stage, with further increases seen in POMC-expressing neurons (Fig. 3F). Notably, our data on DNA methylation across the *POMC* VMR in this in vitro system compare qualitatively and quantitatively with the *POMC* DNA methylation detected during early human embryogenesis (Fig. 3, J and K) (*28*, *29*).

We also evaluated whether *POMC* methylation variability in *POMC*-positive hypothalamic cells would be accompanied by altered *POMC* gene expression. We identified a negative correlation between *POMC* DNA methylation and *POMC* gene expression in this hypothalamic neuronal cell population ($r = -0.39$, $P = 0.013$) (Fig. 3E), indicating that increased *POMC* methylation at CpG positions +1 to +7 is associated with reduced *POMC* gene expression and supporting the functional relevance of *POMC* methylation variability.

However, it has been described in the A^{vy} mouse model that nutritional factors such as carbon-1 (C1) metabolites could alter DNA methylation variability of metastable epialleles during pregnancy (*30*). Therefore, we evaluated whether this scenario could be imitated for *POMC* methylation in this in vitro model.

C1 metabolite availability and *POMC* DNA methylation variability

Previously, we reported correlations between C1 metabolite concentrations at conception in pregnant mothers from the Gambia and *POMC* methylation in their offspring (*12*). C1 metabolism is a pivotal source for the provision of methyl groups for DNA methylation (Fig. 4A) (*31*, *32*). Our experimental setup for the differentiation of naïve cells into POMC$^+$ neurons therefore provided us

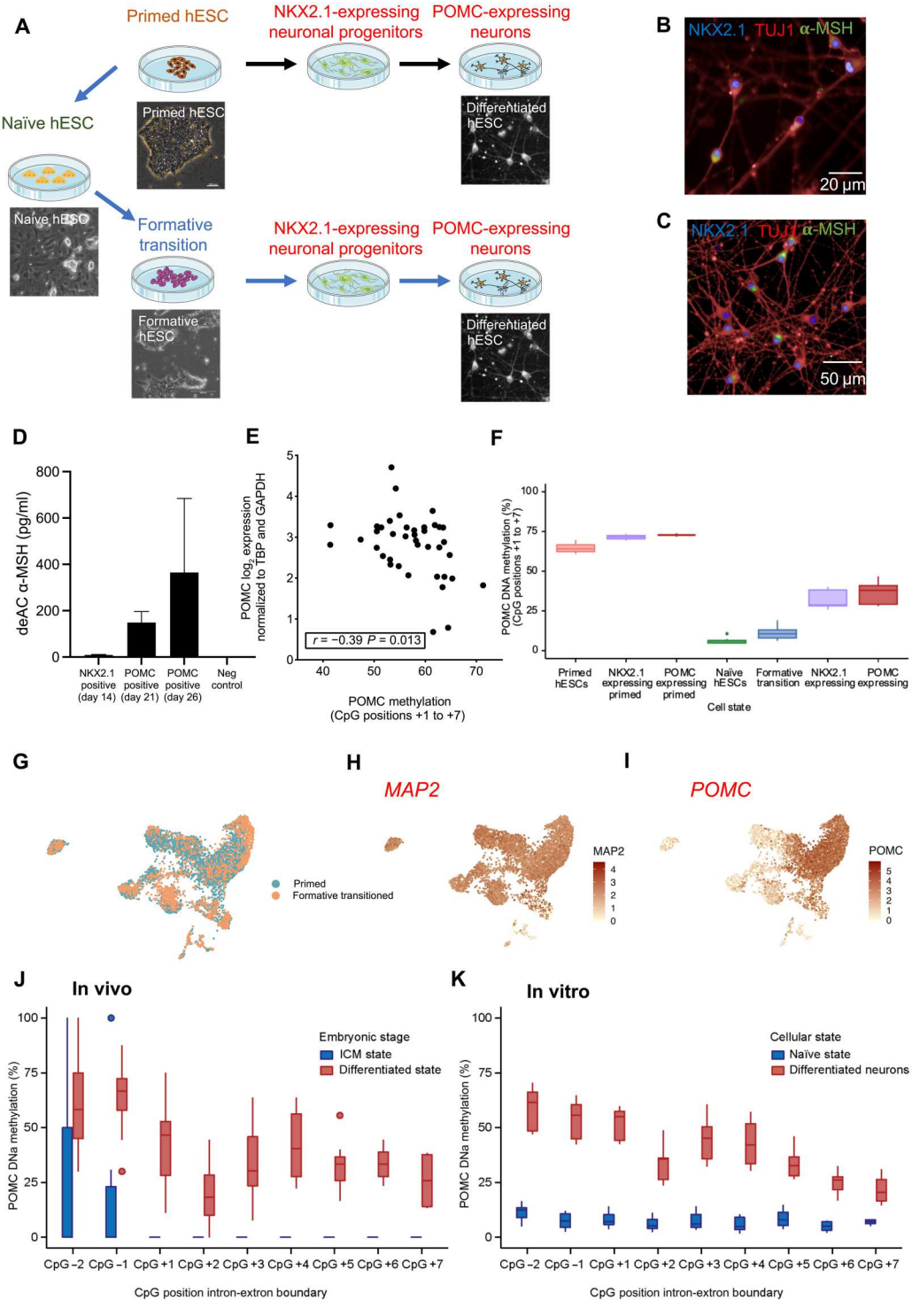

Fig. 3. In vivo and in vitro *POMC* methylation establishment during embryonic development and cell differentiation. (**A**) Overview of the experimental workflow for the hESC-based in vitro model. Primed H1 hESCs were either directly differentiated or transferred into a naïve state. After formative transition, hESCs were differentiated into POMC-expressing neuronal cells. (**B** and **C**) Immunofluorescent overlay imaging of differentiated POMC-expressing cells after costaining with 4′,6-diamidino-2-phenylindole (DAPI) (fig. S5) and antibodies against neuronal markers TUJ1, NKX2.1, and α-MSH. (**D**) Deacetylated α-MSH was measured by tandem mass spectrometry in cell culture supernatant of NKX2.1- and POMC-expressing differentiated neurons. Fresh cell culture media were used as a negative control (n = 3 from three independent experiments). (**E**) *POMC* RNA abundance analyzed by reverse transcription polymerase chain reaction normalized to glyceraldehyde-3-phosphate dehydrogenase (GAPDH) and TATA-binding protein (TBP). *POMC* abundance correlated negatively with *POMC* methylation at *POMC* CpG positions +1 to +7 in the same cell batch (n = 40 from three independent experiments, Pearson correlation coefficient r = −0.39, P = 0.013). Normality was tested with a Shapiro-Wilk test (W = 0.97, P = 0.14). (**F**) *POMC* DNA methylation at CpG positions +1 to +7 in hESC H1 cells that were differentiated into NKX2.1$^+$ progenitors and then into POMC-expressing neurons. This differentiation was performed either starting in the primed (n = 2 from one independent differentiation) or naïve state (n = 15 from three independent differentiations). (**G** to **I**) Single-cell transcriptome analysis of POMC-expressing neuronal cultures at day 26 of differentiation. (G) UMAP (Uniform Manifold Approximation and Projection) plot of 5734 cells colored by cell origin showing intermixing of cells from different origins (primed and formative). (H and I) Feature plots of gene expression for the pan-neuronal marker *MAP2* and for *POMC*. (**J**) Bioinformatic analysis of a whole-genome methylation dataset generated from human embryos (*28*, *29*). *POMC* methylation (CpG positions −2 to +7) was extracted for inner cell mass (ICM) and differentiated embryonic cells. (**K**) hESC *POMC* methylation (CpG positions −2 to +7) in naïve (green) and differentiated (red) states (n = 30 derived from two independent experiments). Data are displayed as median (IQR).

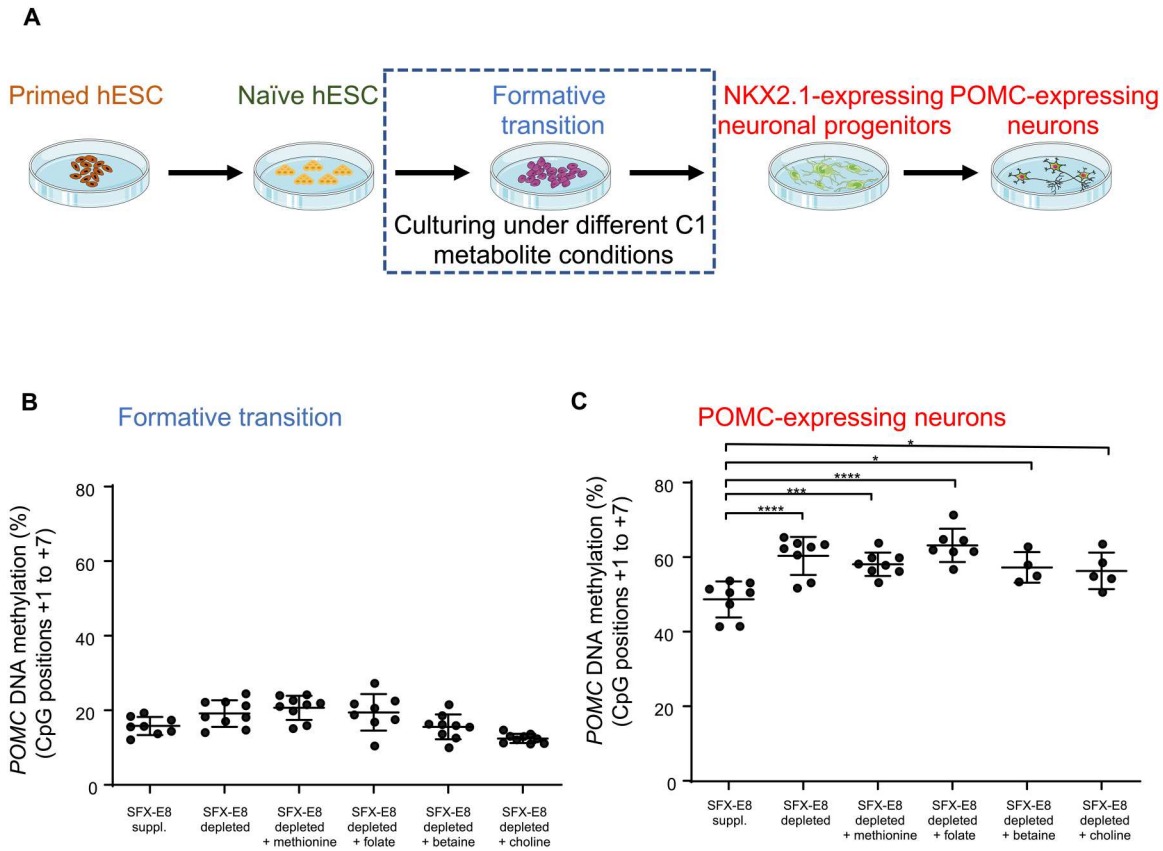

Fig. 4. Relationship between *POMC* methylation variability and C1 metabolite concentrations. (**A**) Schematic of the experimental setup in which C1 metabolite concentrations were modified during the formative transition state (dashed box). hESCs were differentiated into POMC-expressing neurons. (**B**) *POMC* methylation (CpG positions +1 to +7) analyzed at (**B**) formative transition and (**C**) POMC-expressing differentiated cell stages during culture under different conditions of C1 metabolite concentrations: supplemented control E8 medium (SFX-E8 suppl.), depleted medium (SFX-E8 depleted), and depleted E8 media with either added methionine (SFX-E8 depleted + methionine), folate (SFX-E8 depleted + folate), betaine (SFX-E8 depleted + betaine), or choline (SFX-E8 depleted + choline). Samples were compared using one-way ANOVA with supplemental control E8 (SFX-E8 suppl.) as the reference group. Post hoc testing and adjusting were performed with Dunnett's multiple comparison testing (*$P < 0.05$, **$P < 0.01$, ***$P < 0.001$).

with an opportunity to experimentally address the potential role of environmental and nutritional factors on *POMC* methylation establishment in the early embryo.

We cultured naïve cells during their transition into a formative state in E8 medium supplemented with C1 metabolites (SFX-E8/supplemented) and, for comparison, in E8 medium depleted of major C1 metabolites betaine, choline, folate, and methionine (SFX-E8/depleted). Four additional experimental groups were established, with naïve cells cultured during the capacitation period in SFX-E8/depleted medium, to which the specific C1 metabolites methionine, folate, betaine, or choline were individually added (Fig. 4A and fig. S9). Cells cultured under these six conditions were harvested at different developmental stages. Analyses at the formative state showed only a marginal effect of any experimental condition on DNA methylation at the *POMC* locus and in one of two preselected hyper- and hypomethylated control loci (cg06005309 and cg19076425) (Fig. 4B and fig. S10) (*33*). However, analyses of neuronal cultures after 26 days of differentiation showed significantly increased *POMC* DNA methylation in all cultures conducted with SFX-E8/depleted medium, irrespective of the addition of individual C1 metabolites [nested *t* test with different time points as columns (1) and C1 metabolite groups as subcolumns (2), P (1) < 0.0001, P (2) < 0.0001] (Fig. 4C). No such changes in DNA methylation were detected in the hyper- or hypomethylated control regions (fig. S10). Microarray analyses of bulk RNA samples extracted during the capacitation period demonstrated only marginal differences in gene expression profiles between depleted and supplemented media conditions (figs. S11 to S14 and table S2). We observed that samples cultured in supplemented and depleted media with added methionine formed a RNA expression cluster. The samples cultured under depleted conditions with added choline, betaine, and folate shaped a second cluster. We note that the list of differentially expressed genes modified by cell culture conditions (data file S1) contained several key enzymes of C1 metabolism (Fig. 5B, figs. S12 to 14, and table S3). This included the regulation of central C1 enzymes such as *MAT2A* (methionine adenosyltransferase 2A) and *AHCY* (adenoslyhomocysteinase), which are pivotal for the synthesis of *S*-adenosylmethionine (SAM) from methionine, intracellular *S*-adenosyl-L-homocysteine (SAH) regulation, and transmethylation reaction (Fig. 5, B and C), respectively. These gene expression changes are consistent with observations that methionine and SAM are tightly regulated

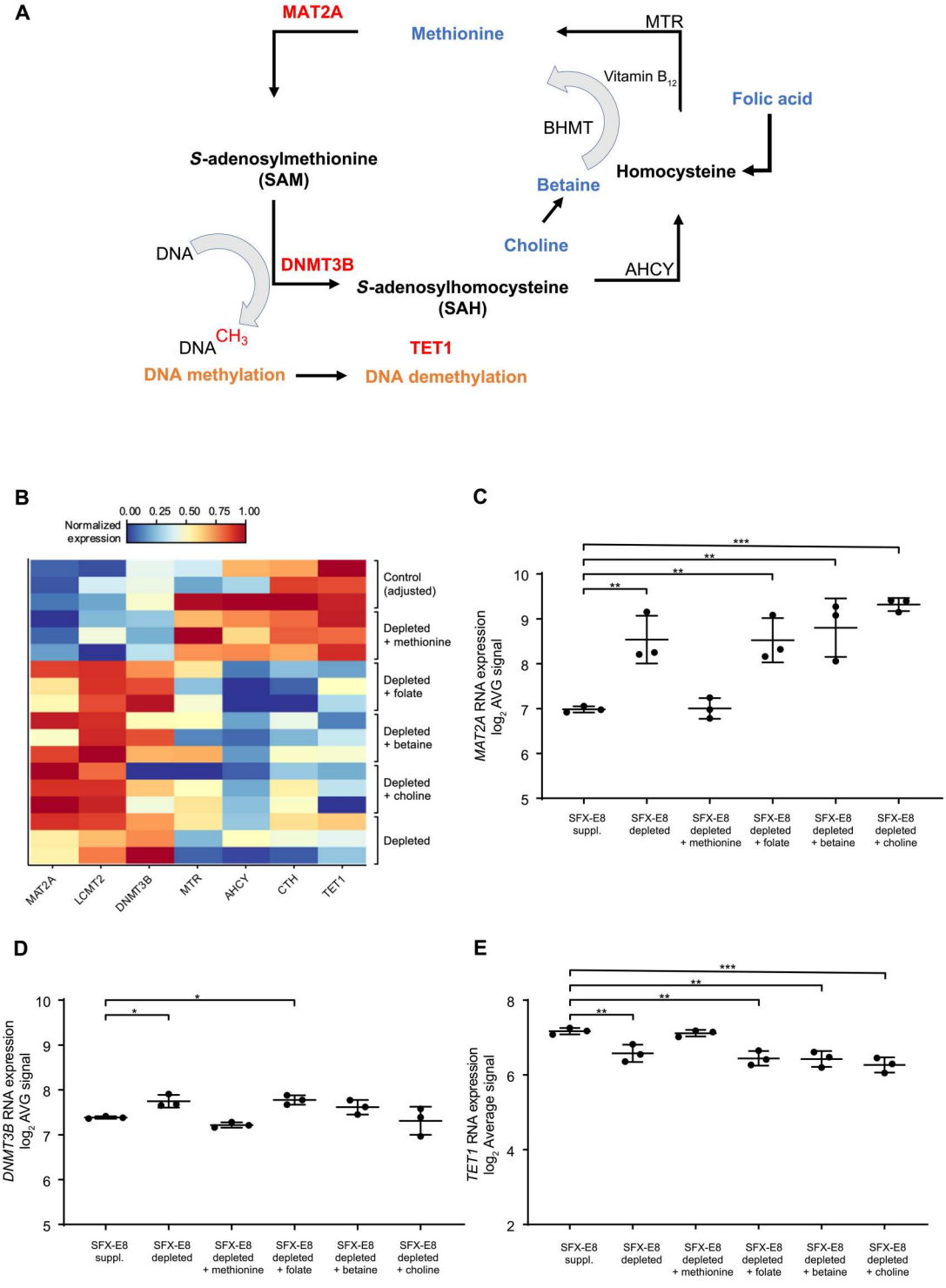

Fig. 5. RNA expression changes of C1 metabolite enzymes during the formative state. (**A**) C1 metabolism pathway is shown. Marked in blue are those metabolites that were added separately during the repriming phase. Marked in red are enzymes for which gene expression changed significantly (ANOVA of C1 metabolite enzymes of interest with subsequent *P* value adjustment for false discovery rate = 0.05) dependent on C1 metabolite conditions. (**B**) Heatmap visualizes RNA expression data of key C1 metabolism enzymes during the formative transition phase under different culturing conditions (SFX-E8 suppl. versus SFX-E8 depleted with added betaine, folate, methionine, or choline). (**C** to **E**) RNA expression (log_2 mean signal) changes of *MAT2A* (**C**), *DNMT3B* (**D**), and *TET1* (**E**) during the formative transition phase ($n = 3$ per condition from three independent experiments) under different conditions of C1 metabolite concentrations. A detailed filtered list of further expression data for genes of interest is provided in the data repository described in the data availability section. MTR, methionine synthase; MAT2A, methionine adenosyltransferase 2 A; AHCY, adenoslyhomocysteinase; BHMT, betaine-homocysteine methyltransferase; DNMT3B, DNA (cytosine-5-)-methyltransferase 3 beta; TET1, Tet methylcytosine dioxygenase 1; LCMT2, leucine carboxyl methyltransferase 2; CTH, cystathionine γ-lyase. *$P < 0.05$, **$P < 0.01$, ***$P < 0.001$, and ****$P < 0.0001$.

in most cell types because SAM affects gene expression and serves as an allosteric regulator of several enzymes required for both methionine and SAM synthesis (*34*, *35*). In addition, and consistent with this clustering, RNA expression of enzymes involved in DNA methylation and demethylation processes [*DNMT3B* (DNA methyltransferase 3 Beta) and *TET1* (ten-eleven translocation methylcytosine dioxygenase 1)] was differentially regulated in opposing directions (Fig. 5, D and E). Our in vitro hESC analysis thus provides evidence of an interrelation between increased *POMC* DNA methylation and gene function within a complex regulated network in which C1 metabolism appears to play a role.

Use of the MC4R agonist setmelanotide as a treatment for patients with obesity and *POMC* hypermethylation

Severe obesity caused by biallelic *POMC* gene mutations is an example of complete α-/β-MSH deficiency, and several patients with this condition have recently been treated with the MC4R agonist setmelanotide in clinical trials approved by the FDA and European Medicines Agency. This intervention reduced the initially persisting hyperphagia and led to a substantial decrease in body weight in POMC-deficient patients (*13*, *36*, *37*). We hypothesized that increased *POMC* methylation might similarly lead to impaired melanocortin pathway function and decreased MSH and that obese invidividuals with *POMC* hypermethylation might therefore benefit from MC4R agonist treatment.

POMC hypermethylation was defined as a methylation score above the 97th percentile based on an analysis of normal-weight individuals. Using this definition, five *POMC*-hypermethylated patients with obesity and severe hyperphagia (one male with Klinefelter syndrome, four females; mean age: 18 ± 5.2 years; mean body weight at baseline: 137.24 ± 34.8 kg; mean BMI at baseline: 43.59 ± 8.56 kg/m^2) (Fig. 6A and table S4A) were enrolled in a phase 2 investigator-initiated study with the MC4R agonist setmelanotide after giving written informed consent (EudraCT no. 2014-002392-28; study protocol provided in data file S2). A monogenic cause for obesity was excluded by genetic testing in these individuals before treatment started. Study participants injected setmelanotide subcutaneously once per day with a mean maximum therapeutic dosage of 2.5 mg (1.0 to 3.0 mg). In summary, after a dose titration phase, patients received the MC4R agonist at the therapeutic dosage [mean of 2.5 mg (1.0 to 3.0 mg)] for 3 months. If a minimal threshold of 5 kg weight loss was achieved, then the patient continued on treatment in an extension phase. This extension treatment phase included a 4-week off-drug period followed by a treatment restart at the therapeutic dosage. Safety parameters were evaluated every 3 months, including cardiovascular, psychological, and dermatological assessments. Patients 1 and 2 discontinued treatment despite weight loss after 64 and 44 weeks, respectively, because they could not make regular site visits because of a new job (patient 1) or compliance could not be further ensured (patient 2).

For all patients, setmelanotide treatment led to a decrease in hunger scores (fig. S15), which was accompanied by a mean reduction of body weight of 7.1 ± 2.32 kg (−5.12 ± 1.11% of prestudy body weight) within the first 3 months (Fig. 6B and fig. S15). One patient lost only 3.2 kg after 13 weeks and therefore did not continue dosing within the extension phase. This patient regained weight after treatment interruption (fig. S15). After a maximum observation period of 38.4 ± 26.0 weeks, the enrolled patients′ mean weight loss was 6.5 ± 3.04 kg (−4.66 ± 2.16% of prestudy body weight; −1.8 ± 1.04 kg/m^2 BMI) compared with baseline body weight. Hunger scores (based on an 11-point Likert scale between 0 to 10 points; 0 = no hunger, 10 = severe hunger) decreased from mean 6.1 ± 1.29 points to 4.8 ± 2.36 points (Fig. 6B and fig. S15). In general, the treatment was well tolerated. No serious adverse event occurred. The most common adverse event was increased pigmentation of skin and nevi (table S4B). This observation relates to cross-activation of MC1R (melanocortin 1 receptor) by the study drug, which is expressed in the skin (*38*). No pathologic changes of blood pressure, heart rate, or safety laboratory values occurred (tables S5 to S7).

DISCUSSION

Obesity and its related comorbidities are associated with major health care problems worldwide. There is a fundamental need to gain new knowledge about individual risk factors and key pathways to improve prevention and to drive therapeutic strategies to reduce obesity prevalence. To this effect, genetic variants captured by polygenic risk scores (*5*) and epigenetic effects including DNA methylation changes have been studied extensively by different groups (*39*). However, tissue specificity, genetic heterogeneity, the potential contribution of environmental/ nutritional factors, and the difficulty of distinguishing causes from consequences have led to difficulties in the interpretation of study results. In this respect, analysis of metastable epialleles has the potential to explain how methylation states established in the early embryo that are longitudinally stable and nontissue-specific affect phenotype variation, as observed for body weight in the A^{vy} mouse model (*11*, *40*–*42*).

In this study, we characterized a VMR in the *POMC* gene by analyzing genotype and methylaton data from twin and large cohort studies. This strengthened existing evidence that the VMR is established during embryonic development and is not genetically determined. This finding is further supported by recently published methylation data from MZ and DZ twin cohorts where monochorionic monoamnionic MZ twins had more highly correlated methylation than dichorionic or monochorionic diamnionic MZ twins (*43*). This indicates the pivotal role of the close amnionic environment and this early embryonic period for the setting of individual methylation signatures.

We observed sex-specific *POMC* methylation, supporting a previous finding in mouse hypothalamic arcuate nucleus and disease-related epigenome-wide association studies, for example, for Alzheimer′s disease (*44*–*46*). The molecular cause for this sexual dimorphism remains elusive and needs to be addressed in future studies. However, the large number of epigenome-wide association studies in which sex-specific methylation has been observed suggests that a complex underlying regulatory mechanism might be at play. We may speculate that this could involve a combination of certain microRNAs, sex-specific histone modification profiles, and hormonal influences.

In our study, elevated *POMC* DNA methylation in females was associated with a 1.4-fold increased risk of developing severe obesity (BMI > 35 kg/m^2). This odds ratio is similar to that observed for one of the most prominent genetic risk variants for weight gain at the fat mass and obesity-associated transcript (*FTO*) gene (rs9939609). Here, homozygous carriers of the A "risk" allele have a 1.67-fold increased risk of developing obesity (*47*).

To further investigate mechanisms underlying the establishment of this *POMC* methylation variant, we established an hESC-based in vitro system. This allowed us to recapitulate early embryonic methylation dynamics in utero and to analyze the relationship between *POMC* DNA methylation, gene expression, and the effect of environmental/nutritional factors. Modification of C1 metabolite concentrations in cell culture media during the formative state was associated with multiple gene expression changes of C1 enzymes and altered *POMC* methylation in the differentiated state. On the basis of this finding, we hypothesize that C1 metabolite modifications during the critical formative state lead to a response at the molecular level, which is consistent with known regulatory mechanisms affecting gene expression and enzyme activity that

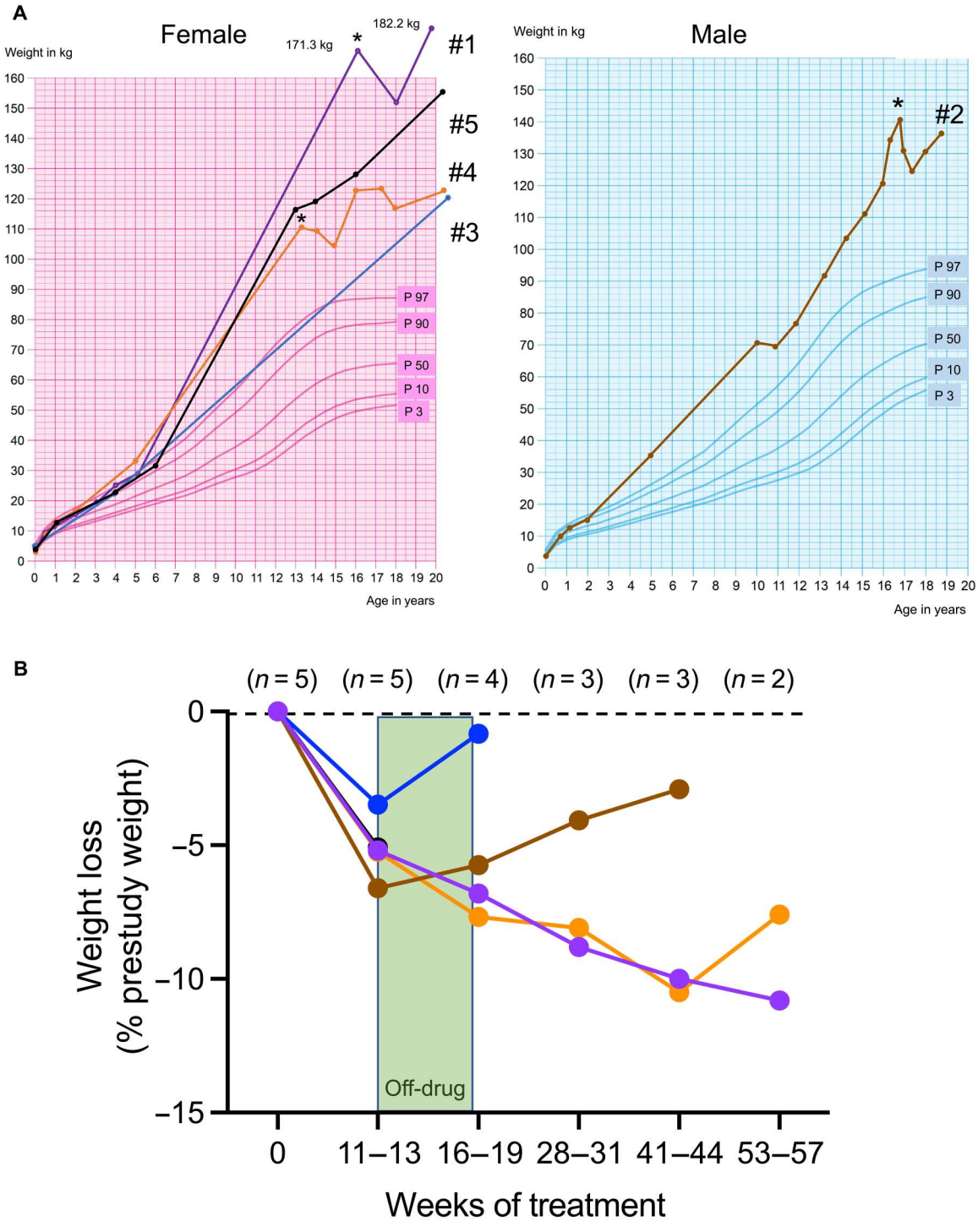

Fig. 6. MC4R agonist treatment leads to reduced body weight in five patients with obesity and *POMC* VMR hypermethylation. (**A**) Prestudy weight course of patients with obesity and increased POMC epigenetic methylation [left: female participants; pink = epigenetic patient 1, blue = epigenetic patient 3, orange = epigenetic patient 4, black = epigenetic patient 5; right: male participant (epigenetic patient 2; brown line)]. Weight trajectory percentiles are calculated on the basis of published data (*55*). * indicates participation in a lifestyle intervention study (*56*). (**B**) Mean body weight change (% weight loss from prestudy body weight with SD) of male and female participants after inclusion in the investigator-initiated study. The green area represents a standardized off-drug phase over 4 weeks. The number of patients included over a specific treatment duration is noted above the graph. Study visits took place regularly every 1 to 3 months, depending on the study phase. The *x* axis represents the visit annotated for each time window in weeks (see data file S2).

tightly control cellular methionine and SAM concentrations (*34*, *35*). This observation points to a complex mechanism regulating DNA methylation and supports a recently published study in which methylation is maintained under the influence of chemical and dietary factors at metastable epialleles in rodents (*48*). Methionine seems to be a key factor in this. It has been shown that increased and decreased methionine in utero may lead to phenotype changes including myelin deficits in mice (*49*) and human birth weight (*50*). In some cell types, DNA methyltransferase activity is a more important regulator of DNA methylation than simply SAM/SAH balance (*51*). Furthermore, SAM/SAH homeostasis in hESCs seems to be stabilized by compensatory up- and down-regulation of RNA expression of intracellular enzymes. Together, these data suggest that both the expression and activity of DNA modifying enzymes such as DNA methyltransferases and enzymes involved in DNA demethylation and the SAM/SAH balance are strong determinants of DNA methylation regulation. The extent to which this system could be modified by external dietary supplementation during pregnancy remains an open question. Folate supplementation during pregnancy is known to reduce the risk of the development of spina bifida (*52*, *53*). It is possible that folate or other metabolite supplementation during this critical period of development might have an impact on *POMC* methylation variation and modify disease risk through subsequent generations. Further studies using this in vitro model including chromatin immunoprecipitation sequencing or assay for transposase-accessible chromatin with sequencing coupled to proteomic and enzyme activity measurements are needed to fully understand the underlying mechanisms involved.

This hESC system additionally allowed us to analyze the functional consequence of increased *POMC* VMR DNA methylation. We observed a negative correlation between *POMC* methylation and decreased *POMC* gene expression in $POMC^{+}$ hypothalamic cells. A similar observation has been made in fat biopsies from obese individuals, with increased *POMC* VMR methylation associated with obesity and *POMC* gene expression inversely correlated with *POMC* methylation (*54*).

Building on these observations, we hypothesized that increased *POMC* methylation leads to altered MSH concentrations and thereby reduces MC4R stimulation within the hypothalamus. This deficit could potentially be substituted with MC4R agonist treatment. To examine this, we enrolled five patients with increased *POMC* methylation scores into an investigator-initiated study of the MC4R agonist setmelanotide. Treatment led to a mean weight reduction of body weight and hunger scores. This study is limited by a small sample size, and a double-blind placebo arm is missing. However, this finding provides evidence for the functional relevance of *POMC* methylation variation and for the need to perform large follow-up studies to gain further knowledge of the extent to which similar patients could benefit from this treatment. In the future, this intervention might be an option as part of a multimodal treatment strategy to stabilize long-lasting weight loss in affected patients with this epigenetic risk variant.

A further limitation of this study is our focus on only one particular metastable epiallele. A broader investigation using methylome-wide analysis with an evaluation of additional epigenetic modifications by analyzing chromatin modifications will be necessary to establish whether our observations are part of a more general mechanism. It would also be of interest to investigate whether similar results could be obtained in additional hESC lines. Furthermore, we focused on five C1 metabilites in our investigation of potential environmental/nutrition influences on *POMC* methylation patterning. It would be of interest to analyze different combinations of altered metabolite concentrations to test the relationship between C1 metabolism and regulation of DNA methylation. Last, hESCs were cultured under modified conditions in the formative state. Changes to the timing and duration of altered C1 metabolite concentrations could provide further insights into critical windows of environmentally induced epigenetic variability.

In summary, we identified evidence that a *POMC* hypermethylation variant is established early in utero and is linked to a sex-specific increased risk of developing obesity later in life. Our hESC in vitro model offers an opportunity to gain insights into factors driving the establishment of regulatory networks of epigenetic marks. This includes the potential to assess the influence of C1 metabolite concentrations and other environmental and nutritional factors with the potential to affect the epigenome. DNA methylation variants at other metastable epialleles affected by this network might contribute cumulatively to an epigenetic risk score that predicts an individual's risk of developing common diseases such as obesity.

MATERIALS AND METHODS

Study design

HNR cohort/GWAS

The sample size for the SNP genome-wide association analysis was chosen to be as large as possible without previous power analysis. Because the hypothesis prespecified was that *POMC* VMR is not influenced by genetic variants, it was important to include as low effects as possible with the available sources. This led to analysis with 1128 or 1083 individuals, respectively, for which Illumina 450 K Methylation Array data or *POMC* pyrosequencing data and genotyping data were available. Additional analysis of the pyrosequenced probes in the context of individuals' BMI was planned. During analysis, we noticed that there was a selection bias for which individuals from the HNR cohort genotyping were performed, leaving severely obese individuals (BMI < 35) underrepresented. Therefore, the study subset was expanded by 300 additional individuals from the HNR cohort. To avoid batch effects, all later performed pyrosequencing was controlled and adjusted with previously analyzed samples. Samples were randomized, and the phenotypic data were blinded from the researcher until the final dataset was fully acquired. Statistical analysis was not blinded. Beside quality of pyrosequencing results, no inclusion or exclusion criteria were applied. Outliers were not excluded because of the large cohort size.

Twin data

The research objective of analyzing DNA methylation of MZ and DZ twins was to evaluate whether MZ twins correlate stronger at the mean DNA methylation of the *POMC* VMR. The *POMC* VMR was tested both in total and at the level of each individual CpG.

Cell culture experiments

Cell culture experiments were exploratory and designed to establish a model to recapitulate de- and remethylation during early in utero development. After the initial results on DNA methylation dynamics, the experiments were extended to perform detailed descriptive

characterization using single-cell RNA sequencing, without intending to compare different conditions. For challenging formative transition with altered C1 metabolite concentration, experimental units were predefined (see below), and every experiment was performed three times independently. After harvesting, the samples were randomized and blinded for further biomolecular analyses. Statistical analyses were performed unblinded.

Clinical study

The clinical study had an explorative approach and aimed to investigate whether patients with obesity and highly methylated *POMC* could in general profit from a therapy with MC4R agonists. Participants were recruited within the obesity outpatient clinic of the Department of Pediatric Endocrinology (Charité–Universitätsmedizin Berlin). Inclusion criteria consisted of obesity (BMI > 30 kg/m^2, BMI-SDS > +2.0) and *POMC* VMR DNA methylation (>51.92% for adults older than 30 years; >35.79% for individuals younger than 30 years). The study was not placebo-controlled. Participants entered a 4-week off-drug phase after a treatment period of 3 months if weight loss of more than 5 kg had been achieved. Thereafter, treatment could be continued at the therapeutic dosage. A detailed description is enclosed in data file S2.

Human cohorts

HNR study cohort

The HNR study is a large population-based cohort study initiated in the year 2000 that has been previously described in detail (*16*). In total, the cohort consists of 4814 males and females who were randomly selected in three German cities (Essen, Mülheim an der Ruhr, and Bochum). Participants were at baseline between 45 and 75 years old. In the present assessment, 1383 samples from the HNR study were analyzed by pyrosequencing for DNA methylation at the POMC VMR (CpG −2 to +7) (table S1). Genome-wide genotype data of pyrosequenced samples were available in 1083 cases, and Illumina 450 K Methylation Array data and genome-wide genotype data were available for 1128 samples and were used for the *POMC* methylation whole-genome association study.

Twin cohorts

Blood samples from 32 pairs of MZ twins and 38 pairs of DZ twins were received from HealthTwist (MZ: 22 female, 42 male, mean BMI of 24.64 ± 3.45 kg/m^2; DZ: 48 female, 28 male, mean BMI of 25.1 ± 4.46 kg/m^2). A total of 37 MZ and 34 DZ samples were analyzed for *PAX8* methylation.

Clinical study

The protocol of this investigator-initiated clinical trial (EudraCT no. 2014-002392-28) is enclosed as supplementary materials (data file S2). The study was approved by the responsible ethical committee (Landesethikkommission Berlin). The obtained data are presented on the basis of a descriptive statistical analysis.

Cell culture

Transfer of hESCs into naïve state

The use of hESC WA01 cells (RRID: CVCL_9771) was approved by the Robert Koch Institut (AZ 3.04.02/0134; AZ 3.04.02/0177). H1 (WA01) hESCs were cultured on Geltrex-coated six-well plates in E8 medium. The medium was changed daily with one double feed per week and was chemically split every 3 to 4 days with 0.5 mM EDTA. Resetting of hESCs (WA01) to a naïve state of pluripotency was performed using standardized NaiveCult from STEMCELL Technologies according to the manufacturer's instructions, which are based on published protocols (*24*). In short, hESCs were cultured under hypoxic conditions (5% O_2, 5% CO_2) on a layer of inactivated mouse embryonic feeder cells (CF-1). For transient histone deacetylase inhibition, valproic acid (STEMCELL Technologies) was used after daily medium change of N2B27 medium supplemented with leukemia inhibitory factor, MAPK kinase inhibitor (PD0325901), glycogen synthase kinase 3 inhibitor (CHIR99021), and protein kinase C inhibitor (Gö6983). After successful transfer into naïve state, homogenous dome-shaped cells were expanded in t2ilGö medium. Enzymatic passaging of cells was performed with TrypLE (Gibco) and supplementation of ROCK inihibitor (Y-27632) for 24 hours to improve cell survival during passaging.

Formative transition of naïve-like stem cells (capacitation)

Naïve H1 (WA01) cells were dissociated with TrypLE, and 1.6 × 10^{4}cells/cm^2 were seeded on Geltrex-coated plates in t2ilGö medium supplemented with 10 μM Y-27632. After 24 hours, the medium was changed to t2ilGö without additional Y-27632. After 48 hours, the culture medium was changed to E8 medium. For further experiments with modification of C1-metabolite concentrations, different E8 media compositions (SFX-E8) were created as described below. Formative transition was performed on the basis of published protocols for a total of 10 to 30 days (*27*).

Modification of C1 metabolite concentrations during the formative transition phase

Concentrations of C1 metabolites in cell culture media were modified during the formative transition phase after hESC H1 cells reached a naïve state. C1 metabolite concentrations of established stem cell media formulations (such as E8) are highly elevated and oversaturated. Therefore, we used a C1 metabolite–depleted Dulbecco's modified Eagle's medium (DMEM) formulation to obtain E8 cell culture media with reduced C1 metabolite concentrations. Because the conventional E8 medium is based on DMEM-F12, and hESCs are not viable in a DMEM-only E8 medium, we used a mixture (1:1) of conventional Ham's F12 medium and DMEM depleted of C1 metabolites (SFX-E8 depleted). The C1-depleted E8 medium had reduced concentrations of folate (1.4 μM), methionine (20 μM), and choline chloride (50 μM) compared with the conventionally used E8 medium compositions. C1-depleted E8 (SFX-E8 depleted) was used as the basal medium during cell culturing in the formative phase. To analyze the impact of C1 metabolites, each C1 metabolite (folate, choline, methionine, and betaine) was added separately to SFX-E8–depleted media. As an adjusted control group, we created a basal medium with fully supplemented C1 metabolites as in conventional E8 cell culture media (based on depleted formulation; SFX-E8 supplemented). The change in morphology, viability, and cell growth during the protocol was controlled by performing formative transition in conventional E8 medium in parallel. Therefore, the following media compositions were used: C1-depleted E8 medium with added 1000 μM methionine (SFX-E8 depleted + methionine), C1-depleted E8 medium with added 6 μM folate (SFX-E8 depleted + folate), C1-depleted E8 medium with added 450 μM betaine (SFX-E8 depleted + betaine), C1-depleted E8 medium with added 640 μM choline chloride (SFX-E8 depleted + choline), and fully supplemented E8 media (SFX-E8 depleted + supplemented).

Differentiation into POMC-expressing neurons

Differentiation of hESCs to hypothalamic-like neurons was conducted according to published protocols (*20*, *21*). hESC H1 cells

were seeded on Geltrex-coated culture ware in E8 media and cultured until confluence. Subsequently, neuroectodermal induction was initiated by media changed to knock out serum replacement medium (Gibco) with supplementation of 10 μM SB 431542 (Selleckchem) and 2.5 μM LDN 193189 (Selleckchem), whereas ventralization was induced by simultaneous supplementation of SHH (sonic hedgehog) (100 ng/ml; R&D Systems) and 2 μM purmorphamine (Stemolecule) for 8 days. Further differentiation into NKX2.1-expressing progenitor cells was reached by Notch inhibition (DAPT, Tocris) starting on day 9. For further differentiation, $1 \times 10^5/cm^2$ cells were replated on day 13 on poly-L-ornithine/laminine–coated plates in N2B27 medium with DAPT and later brain-derived neurotrophic factor (R&D Systems) addition. POMC-expressing neurons were harvested or fixed for staining on day 26.

Analysis of human in vivo DNA methylation from embryonic tissue

Methylation data from Guo *et al.* (*28*) were downloaded from Gene Expression Omnibus (GEO) (accession number GSE49828), including reduced representation bisulfite sequencing data for ICM and post-implantation embryos. In addition, whole genome-wide bisulfite sequencing data were available for ICM and liver. Post-bisulfite adapter tagging data from Zhu *et al.* (*29*) were accessed and downloaded from GEO (accession number GSE81233) for samples derived from ICM at 7 and 9 weeks. Furthermore, the data were available derived from heart tissue at 11 weeks. The data were filtered by Git Bash for Chr2: 25383722–25391559 (hg19) and subsequently analyzed and visualized in R. The minimum CpG coverage was set to five, and samples were assigned to three different developmental stages: ICM, post-implantation, and differentiated samples (embryonic heart and liver).

Statistical analysis

In cell culture experiments, cells from one culture dish were defined as experimental units; for example, differentiated neurons from one six-well plate were dissociated, resuspended, and harvested as two cell pellets for DNA and RNA analysis of one experimental unit. Each formative and differentiation experiment was repeated at least three times, conducting the complete protocol starting from the naïve state. Sub-step repetition, for example, repeated differentiation from the same stock of formative cells, was not regarded as an independent experiment. Statistical tests were performed with biological units (indicated as n for each test and graph). Unless otherwise indicated, the data are presented as means ± SD in all graphs. For all tests performed, normality was confirmed with Shapiro-Wilk test ($P > 0.05$ was assumed normally distributed) and visual evaluation of Q-Q plots. If data were not normally distributed, then a Krukal-Wallis test instead of analysis of variance (ANOVA) was performed. For all other parametric tests (Pearson's correlation and Student's t test), samples fulfilled assumptions, and no non-parametric tests were used. On the basis of the central limits theorem (for all $n > 100$ per group), it was assumed that samples are well approximated with normal distribution even if the data values are not normally distributed. Assumption of homoscedasticity was checked by plotting normal Q-Q plots and diagnostic plots showing the distribution of residuals, where mean of residuals was supposed to be 0 without outliers and evenly distributed for different groups. To analyze the expression of C1 metabolism–related genes, the RNA array data were filtered for a list of genes of interest containing all genes. For visualizing the data in a heatmap, an empirical normalization transformation was performed, bringing the data to the 0 to 1 scale by subtracting the minimum and dividing by the maximum of all observations. Considering that all raw values of these genes were visible to the scientist, statistical testing shown in Fig. 5 was adjusted not only for multiple testing within each shown one-way ANOVA but also for all genes of this list with a false discovery rate of 0.05. In detail, all genes passed the Shapiro-Wilk normality test for each C1 metabolite group. However, for AHCY and SHMT1, at least one group failed normal distribution. In this case, Kruskal-Wallis with subsequent uncorrected Dunn's test was performed. Otherwise, we performed a one-way ANOVA for each gene with "control (adjusted)" as a reference group with Fisher's uncorrected least significant difference test as post hoc test and created a stack of all 55 P values, which was then analyzed with the two-stage linear step-up procedure of Benjamini, Krieger, and Yekutieli. This led to 19 discoveries, which are listed in the data repository described in the data and materials availability section.

Supplementary Materials

This PDF file includes:
Materials and Methods
Figs. S1 to S15
Tables S1 to S7

Other Supplementary Material for this manuscript includes the following:
Data files S1 and S2
MDAR Reproducibility Checklist

View/request a protocol for this paper from *Bio-protocol*.

REFERENCES AND NOTES

1. WHO, *Report: Fiscal Policies for Diet and Prevention of Noncommunicable Diseases* (WHO, 2016).
2. WHO, *Global action plan on physical activity 2018–2030: More active people for a healthier world 2019* (WHO, 2018).
3. H. H. Maes, M. C. Neale, L. J. Eaves, Genetic and environmental factors in relative body weight and human adiposity. *Behav. Genet.* **27**, 325–351 (1997).
4. A. A. van der Klaauw, I. S. Farooqi, The hunger genes: Pathways to obesity. *Cell* **161**, 119–132 (2015).
5. A. V. Khera, M. Chaffin, K. H. Wade, S. Zahid, J. Brancale, R. Xia, M. Distefano, O. Senol-Cosar, M. E. Haas, A. Bick, K. G. Aragam, E. S. Lander, G. D. Smith, H. Mason-Suares, M. Fornage, M. Lebo, N. J. Timpson, L. M. Kaplan, S. Kathiresan, Polygenic prediction of weight and obesity trajectories from birth to adulthood. *Cell* **177**, 587–596.e9 (2019).
6. E. E. Eichler, J. Flint, G. Gibson, A. Kong, S. M. Leal, J. H. Moore, J. H. Nadeau, Missing heritability and strategies for finding the underlying causes of complex disease. *Nat. Rev. Genet.* **11**, 446–450 (2010).
7. I. Panzeri, J. A. Pospisilik, Epigenetic control of variation and stochasticity in metabolic disease. *Mol. Metab.* **14**, 26–38 (2018).
8. R. A. Koza, L. Nikonova, J. Hogan, J. S. Rim, T. Mendoza, C. Faulk, J. Skaf, L. P. Kozak, Changes in gene expression foreshadow diet-induced obesity in genetically identical mice. *PLOS Genet.* **2**, e81 (2006).
9. M. M. Dickies, A new viable yellow mutation in the house mouse. *J. Hered.* **53**, 84–86 (1962).
10. T. J. Vasicek, L. Zeng, X. J. Guan, T. Zhang, F. Costantini, S. M. Tilghman, Two dominant mutations in the mouse fused gene are the result of transposon insertions. *Genetics* **147**, 777–786 (1997).
11. V. K. Rakyan, M. E. Blewitt, R. Druker, J. I. Preis, E. Whitelaw, Metastable epialleles in mammals. *Trends Genet.* **18**, 348–351 (2002).
12. P. Kühnen, D. Handke, R. A. Waterland, B. J. Hennig, M. Silver, A. J. Fulford, P. Dominguez-Salas, S. E. Moore, A. M. Prentice, J. Spranger, A. Hinney, J. Hebebrand, F. L. Heppner, L. Walzer, C. Grötzinger, J. Gromoll, S. Wiegand, A. Gruters, H. Krude, Interindividual

variation in DNA methylation at a putative POMC metastable epiallele is associated with obesity. *Cell Metab.* **24**, 502–509 (2016).
13. K. Clément, E. van den Akker, J. Argente, A. Bahm, W. K. Chung, H. Connors, K. De Waele, I. S. Farooqi, J. Gonneau-Lejeune, G. Gordon, K. Kohlsdorf, C. Poitou, L. Puder, J. Swain, M. Stewart, G. Yuan, M. Wabitsch, P. Kühnen; Setmelanotide POMC and LEPR Phase 3 Trial Investigators, Efficacy and safety of setmelanotide, an MC4R agonist, in individuals with severe obesity due to LEPR or POMC deficiency: Single-arm, open-label, multicentre, phase 3 trials. *Lancet Diabetes Endocrinol.* **8**, 960–970 (2020).
14. P. Kuehnen, M. Mischke, S. Wiegand, C. Sers, B. Horsthemke, S. Lau, T. Keil, Y.-A. Lee, A. Grueters, H. Krude, An Alu element-associated hypermethylation variant of the POMC gene is associated with childhood obesity. *PLOS Genet.* **8**, e1002543 (2012).
15. S. Voisin, M. S. Almén, G. Y. Zheleznyakova, L. Lundberg, S. Zarei, S. Castillo, F. E. Eriksson, E. K. Nilsson, M. Blüher, Y. Böttcher, P. Kovacs, J. Klovins, M. Rask-Andersen, H. B. Schiöth, Many obesity-associated SNPs strongly associate with DNA methylation changes at proximal promoters and enhancers. *Genome Med.* **7**, 103 (2015).
16. A. Schmermund, S. Mohlenkamp, A. Stang, D. Gronemeyer, R. Seibel, H. Hirche, K. Mann, W. Siffert, K. Lauterbach, J. Siegrist, K. H. Jockel, R. Erbel, Assessment of clinically silent atherosclerotic disease and established and novel risk factors for predicting myocardial infarction and cardiac death in healthy middle-aged subjects: Rationale and design of the Heinz Nixdorf RECALL Study. Risk Factors, Evaluation of Coronary Calcium and Lifestyle. *Am. Heart J.* **144**, 212–218 (2002).
17. T. E. Van Baak, C. Coarfa, P. A. Dugue, G. Fiorito, E. Laritsky, M. S. Baker, N. J. Kessler, J. Dong, J. D. Duryea, M. J. Silver, A. Saffari, A. M. Prentice, S. E. Moore, A. Ghantous, M. N. Routledge, Y. Y. Gong, Z. Herceg, P. Vineis, G. Severi, J. L. Hopper, M. C. Southey, G. G. Giles, R. L. Milne, R. A. Waterland, Epigenetic supersimilarity of monozygotic twin pairs. *Genome Biol.* **19**, 2 (2018).
18. C. J. Gunasekara, C. A. Scott, E. Laritsky, M. S. Baker, H. MacKay, J. D. Duryea, N. J. Kessler, G. Hellenthal, A. C. Wood, K. R. Hodges, M. Gandhi, A. B. Hair, M. J. Silver, S. E. Moore, A. M. Prentice, Y. Li, R. Chen, C. Coarfa, R. A. Waterland, A genomic atlas of systemic interindividual epigenetic variation in humans. *Genome Biol.* **20**, 105 (2019).
19. M. J. Silver, A. Saffari, N. J. Kessler, G. R. Chandak, C. H. D. Fall, P. Issarapu, A. Dedaniya, M. Betts, S. E. Moore, M. N. Routledge, Z. Herceg, C. Cuenin, M. Derakhshan, P. T. James, D. Monk, A. M. Prentice, Environmentally sensitive hotspots in the methylome of the early human embryo. *eLife* **11**, e72031 (2022).
20. L. Wang, K. Meece, D. J. Williams, K. A. Lo, M. Zimmer, G. Heinrich, J. Martin Carli, C. A. Leduc, L. Sun, L. M. Zeltser, M. Freeby, R. Goland, S. H. Tsang, S. L. Wardlaw, D. Egli, R. L. Leibel, Differentiation of hypothalamic-like neurons from human pluripotent stem cells. *J. Clin. Invest.* **125**, 796–808 (2015).
21. L. Wang, D. Egli, R. L. Leibel, Efficient generation of hypothalamic neurons from human pluripotent stem cells. *Curr. Protoc. Hum. Genet.* **90**, 21.5.1–21.5.14 (2016).
22. P. Kirwan, R. G. Kay, B. Brouwers, V. Herranz-Perez, M. Jura, P. Larraufie, J. Jerber, J. Pembroke, T. Bartels, A. White, F. M. Gribble, F. Reimann, I. S. Farooqi, S. O'Rahilly, F. T. Merkle, Quantitative mass spectrometry for human melanocortin peptides in vitro and in vivo suggests prominent roles for β-MSH and desacetyl α-MSH in energy homeostasis. *Mol. Metab.* **17**, 82–97 (2018).
23. T. Nakamura, I. Okamoto, K. Sasaki, Y. Yabuta, C. Iwatani, H. Tsuchiya, Y. Seita, S. Nakamura, T. Yamamoto, M. Saitou, A developmental coordinate of pluripotency among mice, monkeys and humans. *Nature* **537**, 57–62 (2016).
24. G. Guo, F. von Meyenn, M. Rostovskaya, J. Clarke, S. Dietmann, D. Baker, A. Sahakyan, S. Myers, P. Bertone, W. Reik, K. Plath, A. Smith, Epigenetic resetting of human pluripotency. *Development* **144**, 2748–2763 (2017).
25. G. Guo, F. von Meyenn, F. Santos, Y. Chen, W. Reik, P. Bertone, A. Smith, J. Nichols, Naive pluripotent stem cells derived directly from isolated cells of the human inner cell mass. *Stem Cell Rep.* **6**, 437–446 (2016).
26. G. G. Stirparo, T. Boroviak, G. Guo, J. Nichols, A. Smith, P. Bertone, Integrated analysis of single-cell embryo data yields a unified transcriptome signature for the human pre-implantation epiblast. *Development* **145**, dev158501 (2018).
27. M. Rostovskaya, G. G. Stirparo, A. Smith, Capacitation of human naïve pluripotent stem cells for multi-lineage differentiation. *Development* **146**, dev172916 (2019).
28. H. Guo, P. Zhu, L. Yan, R. Li, B. Hu, Y. Lian, J. Yan, X. Ren, S. Lin, J. Li, X. Jin, X. Shi, P. Liu, X. Wang, W. Wang, Y. Wei, X. Li, F. Guo, X. Wu, X. Fan, J. Yong, L. Wen, S. X. Xie, F. Tang, J. Qiao, The DNA methylation landscape of human early embryos. *Nature* **511**, 606–610 (2014).
29. P. Zhu, H. Guo, Y. Ren, Y. Hou, J. Dong, R. Li, Y. Lian, X. Fan, B. Hu, Y. Gao, X. Wang, Y. Wei, P. Liu, J. Yan, X. Ren, P. Yuan, Y. Yuan, Z. Yan, L. Wen, L. Yan, J. Qiao, F. Tang, Single-cell DNA methylome sequencing of human preimplantation embryos. *Nat. Genet.* **50**, 12–19 (2018).
30. R. A. Waterland, D. C. Dolinoy, J. R. Lin, C. A. Smith, X. Shi, K. G. Tahiliani, Maternal methyl supplements increase offspring DNA methylation at Axin Fused. *Genesis* **44**, 401–406 (2006).
31. P. James, S. Sajjadi, A. S. Tomar, A. Saffari, C. H. D. Fall, A. M. Prentice, S. Shrestha, P. Issarapu, D. K. Yadav, L. Kaur, K. Lillycrop, M. Silver, G. R. Chandak; E. s. group, Candidate genes linking maternal nutrient exposure to offspring health via DNA methylation: A review of existing evidence in humans with specific focus on one-carbon metabolism. *Int. J. Epidemiol.* **47**, 1910–1937 (2018).
32. G. S. Ducker, J. D. Rabinowitz, One-carbon metabolism in health and disease. *Cell Metab.* **25**, 27–42 (2017).
33. M. Derakhshan, N. J. Kessler, M. Ishida, C. Demetriou, N. Brucato, G. E. Moore, C. H. D. Fall, G. R. Chandak, F.-X. Ricaut, A. M. Prentice, G. Hellenthal, M. J. Silver, Tissue- and ethnicity-independent hypervariable DNA methylation states show evidence of establishment in the early human embryo. *Nucleic Acids Res.* **50**, 6735–6752 (2022).
34. J. M. Mato, M. L. Martinez-Chantar, S. C. Lu, Methionine metabolism and liver disease. *Annu. Rev. Nutr.* **28**, 273–293 (2008).
35. A. M. Scarborough, J. N. Flaherty, O. V. Hunter, K. Liu, A. Kumar, C. Xing, B. P. Tu, N. K. Conrad, SAM homeostasis is regulated by CFI_m-mediated splicing of MAT2A. *eLife* **10**, e64930 (2021).
36. K. Clement, H. Biebermann, I. S. Farooqi, L. Van der Ploeg, B. Wolters, C. Poitou, L. Puder, F. Fiedorek, K. Gottesdiener, G. Kleinau, N. Heyder, P. Scheerer, U. Blume-Peytavi, I. Jahnke, S. Sharma, J. Mokrosinski, S. Wiegand, A. Muller, K. Weiss, K. Mai, J. Spranger, A. Gruters, O. Blankenstein, H. Krude, P. Kuhnen, MC4R agonism promotes durable weight loss in patients with leptin receptor deficiency. *Nat. Med.* **24**, 551–555 (2018).
37. P. Kuhnen, K. Clement, S. Wiegand, O. Blankenstein, K. Gottesdiener, L. L. Martini, K. Mai, U. Blume-Peytavi, A. Gruters, H. Krude, Proopiomelanocortin deficiency treated with a melanocortin-4 receptor agonist. *N. Engl. J. Med.* **375**, 240–246 (2016).
38. V. Kanti, L. Puder, I. Jahnke, P. M. Krabusch, J. Kottner, A. Vogt, C. Richter, A. Andruck, L. Lechner, C. Poitou, H. Krude, K. Gottesdiener, K. Clement, I. S. Farooqi, S. Wiegand, P. Kuhnen, U. Blume-Peytavi, A melanocortin-4 receptor agonist induces skin and hair pigmentation in patients with monogenic mutations in the leptin-melanocortin pathway. *Skin Pharmacol. Physiol.* **34**, 307–316 (2021).
39. C. G. Bell, The epigenomic analysis of human obesity. *Obesity* **25**, 1471–1481 (2017).
40. K. Dalgaard, K. Landgraf, S. Heyne, A. Lempradl, J. Longinotto, K. Gossens, M. Ruf, M. Orthofer, R. Strogantsev, M. Selvaraj, T. T. Lu, E. Casas, R. Teperino, M. A. Surani, I. Zvetkova, D. Rimmington, Y. C. Tung, B. Lam, R. Larder, G. S. Yeo, S. O'Rahilly, T. Vavouri, E. Whitelaw, J. M. Penninger, T. Jenuwein, C. L. Cheung, A. C. Ferguson-Smith, A. P. Coll, A. Korner, J. A. Pospisilik, Trim28 haploinsufficiency triggers Bi-stable epigenetic obesity. *Cell* **164**, 353–364 (2016).
41. A. Kazachenka, T. M. Bertozzi, M. K. Sjoberg-Herrera, N. Walker, J. Gardner, R. Gunning, E. Pahita, S. Adams, D. Adams, A. C. Ferguson-Smith, Identification, characterization, and heritability of murine metastable epialleles: Implications for non-genetic inheritance. *Cell* **175**, 1717 (2018).
42. C. J. Gunasekara, R. A. Waterland, A new era for epigenetic epidemiology. *Epigenomics* **11**, 1647–1649 (2019).
43. J. van Dongen, S. D. Gordon, A. F. McRae, V. V. Odintsova, H. Mbarek, C. E. Breeze, K. Sugden, S. Lundgren, J. E. Castillo-Fernandez, E. Hannon, T. E. Moffitt, F. A. Hagenbeek, C. E. M. van Beijsterveldt, J. J. Hottenga, P.-C. Tsai; BIOS Consortium; Genetics of DNA Methylation Consortiom, J. L. Min, G. Hemani, E. A. Ehli, F. Paul, C. D. Stern, B. T. Heijmans, P. E. Slagboom, L. Daxinger, S. M. van der Maarel, E. J. C. de Geus, G. Willemsen, G. W. Montgomery, B. Reversade, M. Ollikainen, J. Kaprio, T. D. Spector, J. T. Bell, J. Mill, A. Caspi, N. G. Martin, D. I. Boomsma, Identical twins carry a persistent epigenetic signature of early genome programming. *Nat. Commun.* **12**, 5618 (2021).
44. R. H. Mulder, A. Neumann, C. A. M. Cecil, E. Walton, L. C. Houtepen, A. J. Simpkin, J. Rijlaarsdam, B. T. Heijmans, T. R. Gaunt, J. F. Felix, V. W. V. Jaddoe, M. J. Bakermans-Kranenburg, H. Tiemeier, C. L. Relton, M. H. van IJzendoorn, M. Suderman, Epigenome-wide change and variation in DNA methylation in childhood: Trajectories from birth to late adolescence. *Hum. Mol. Genet.* **30**, 119–134 (2021).
45. L. Zhang, J. I. Young, L. Gomez, T. C. Silva, M. A. Schmidt, J. Cai, X. Chen, E. R. Martin, L. Wang, Sex-specific DNA methylation differences in Alzheimer's disease pathology. *Acta Neuropathol. Commun.* **9**, 77 (2021).
46. H. MacKay, C. J. Gunasekara, K. Y. Yam, D. Srisai, H. K. Yalamanchili, Y. Li, R. Chen, C. Coarfa, R. A. Waterland, Sex-specific epigenetic development in the mouse hypothalamic arcuate nucleus pinpoints human genomic regions associated with body mass index. *Sci. Adv.* **8**, eabo3991 (2022).
47. T. M. Frayling, N. J. Timpson, M. N. Weedon, E. Zeggini, R. M. Freathy, C. M. Lindgren, J. R. Perry, K. S. Elliott, H. Lango, N. W. Rayner, B. Shields, L. W. Harries, J. C. Barrett, S. Ellard, C. J. Groves, B. Knight, A. M. Patch, A. R. Ness, S. Ebrahim, D. A. Lawlor, S. M. Ring, Y. Ben-Shlomo, M. R. Jarvelin, U. Sovio, A. J. Bennett, D. Melzer, L. Ferrucci, R. J. Loos, I. Barroso, N. J. Wareham, F. Karpe, K. R. Owen, L. R. Cardon, M. Walker, G. A. Hitman, C. N. Palmer, A. S. Doney, A. D. Morris, G. D. Smith, A. T. Hattersley, M. I. McCarthy, A common variant in the FTO gene is associated with body mass index and predisposes to childhood and adult obesity. *Science* **316**, 889–894 (2007).
48. T. M. Bertozzi, J. L. Becker, G. E. T. Blake, A. Bansal, D. K. Nguyen, D. S. Fernandez-Twinn, S. E. Ozanne, M. S. Bartolomei, R. A. Simmons, E. D. Watson, A. C. Ferguson-Smith, Variably

methylated retrotransposons are refractory to a range of environmental perturbations. *Nat. Genet.* **53**, 1233–1242 (2021).
49. X. Chen, N. X. Huang, Y. J. Cheng, Q. Y. Cai, Y. P. Tian, X. S. Chen, L. Xiao, DNA hypermethylation induced by L-methionine leads to oligodendroglial and myelin deficits and schizophrenia-like behaviors in adolescent mice. *Front. Neurosci.* **15**, 659853 (2021).
50. A. L. Monsen, J. Schneede, P. M. Ueland, Mid-trimester amniotic fluid methionine concentrations: A predictor of birth weight and length. *Metabolism* **55**, 1186–1191 (2006).
51. J. Perla-Kajan, H. Jakubowski, Dysregulation of epigenetic mechanisms of gene expression in the pathologies of hyperhomocysteinemia. *Int. J. Mol. Sci.* **20**, (2019).
52. N. C. Nevin, M. J. Seller, Prevention of neural-tube-defect recurrences. *Lancet* **335**, 178–179 (1990).
53. A. E. Czeizel, I. Dudas, Prevention of the first occurrence of neural-tube defects by periconceptional vitamin supplementation. *N. Engl. J. Med.* **327**, 1832–1835 (1992).
54. N. K. Sharma, M. E. Comeau, D. Montoya, M. Pellegrini, T. D. Howard, C. D. Langefeld, S. K. Das, Integrative analysis of glucometabolic traits, adipose tissue DNA methylation, and gene expression identifies epigenetic regulatory mechanisms of insulin resistance and obesity in African Americans. *Diabetes* **69**, 2779–2793 (2020).
55. M. W. Kromeyer-Hauschild, D. Kunze, F. Geller, H. C. Geiß, V. Hesse, A. von Hippel, U. Jaeger, D. Johnsen, W. Korte, K. Menner, G. Müller, J. M. Müller, A. Niemann- Pilatus, T. Remer, F. Schaefer, H.-U. Wittchen, S. Zabransky, K. Zellner, A. Ziegler, J. Hebebrand, Perzentile für den Body-mass-Index für das Kindes- und Jugendalter unter Heranziehung verschiedener deutscher Stichproben. *Monatszeitschr. Kinderh.* **149**, 807–818 (2001).
56. A. M. Bau, A. Ernert, H. Krude, S. Wiegand, Hormonal regulatory mechanisms in obese children and adolescents after previous weight reduction with a lifestyle intervention: Maintain - paediatric part - a RCT from 2009-15. *BMC Obes.* **3**, 29 (2016).

Acknowledgments: We thank A. Stielow, L. Puder, R. Öltjen, L. Usadel, L. Ruck, D. Sebinger, C. Doege, C. Sers, M. Derakshan, T. Elsholz, F. Böhringer, and the BIH Core Unit Stem Cells and Organoids. Rhythm Pharmaceuticals provided the study drug and regulatory support. Scientific figure illustrations were created using images adapted from Servier Medical Art by Servier (www.servier.com). **Funding:** This work was funded by the Germany Research Foundation (DFG) KU 2673/6-1, KU 2673/7-1, CRC1423/B02 (to P. Kühnen), CRC296/ P04 (to P. Kühnen), KU 2673/2-2 (to P. Kühnen), ERC CoG 101043991 (E-VarEndo, to P. Kühnen); BIH SPARK validation fund track 2 (to P. Kühnen); BIH Charité Junior Clinician Scientist Program (to P.M. Krabusch); BIH MD Student Research Stipends (to L.L.); Klaus-Kruse scholarship (German Society for Pediatric Endocrinology and Diabetology) (to P. Kühnen); and BIH MD Student Research Stipends (to L.L.). **Author contributions:** P.K. conceptualized and supervised the study. P.K., L.L., H.S., A.M.P., M.J.S., M.S.F., B.H., and V.F.V. designed the experiments. L.L. and V.F.V. performed experiments. HNR cohort samples were provided by B.H., E.L., C.S., K.-H.J., B.S., M.M.N., P.H., and S.H. Formal analysis was performed by L.L., R.O., C.S., E.L., K.J., M.M.N., B.O., M.M. and P.K.. P.K., S.W., P.M.K., U.B.-P., K.W., K.M., O.B., and P.W.K. performed the clinical trial. P.K. prepared the original draft of manuscript. The manuscript has been reviewed and edited by P.K., L.L., R.O., M.J.S., A.M.P., M.S.F., and B.H. All authors provided critical feedback. **Competing interests:** P.W.K. is an employee of Rhythm Pharmaceuticals. P.K. received consultation fee once and has been invited to hold talks from Rhythm Pharmaceuticals. All other authors declare that they have no competing interests. Charité-Universitätsmedizin Berlin is a study site for Rhythm-sponsored clinical trials [patent: WO 2017/059076 (Method of treating melanocortin-4 receptor pathway-asociated disorders)]. **Data and materials availability:** All data associated with this study are in the paper or in the Supplementary Materials. Correspondence and requests for materials should be addressed to P.K. R code used to analyze and visualize data, primer sequences, detailed statistical analysis, as well as the RNA array and single-cell RNA-seq data generated in this study are publicly available at 10.5281/zenodo.7657392.

Submitted 12 December 2022
Accepted 22 June 2023
Published 19 July 2023
10.1126/scitranslmed.adg1659